

Patent
703538.4027

IN THE UNITED STATES PATENT AND TRADEMARK OFFICE

Appl. No. : 10/751,131 Confirmation No.: 1733
Applicant : Bedri Cetiner et al.
Filing Date : December 31, 2003
Title : RF MEMS FABRICATION ON A LAMINATED SUBSTRATE
Group Art Unit : 2821
Examiner : Phan, Tho Gia
Docket No. : 703538.4027
Customer No. : 34313

DECLARATION UNDER 37 CFR § 1.131

Mail Stop Amendment
Commissioner for Patents
P. O. Box 1450
Alexandria, VA 22313-1450

Sir:

We, Bedri A. Cetiner, Mark Bachman, Guann-Pyng Li, Jiangyuan Qian, Hung-Pin Chang, and Franco De Flaviis, do declare and state as follows:

1. We have personal knowledge of the matters set forth herein and, if called as a witness, could and would testify competently thereto. Those matters set forth on information and belief are believed to be true.
2. We are the only named joint inventors of the above-identified patent application, U.S. Non-Provisional Patent Application Serial No. 10/751,131, filed December 31, 2003, which claims priority to the Provisional Patent Application Serial No. 60/437,209, filed December 31, 2002.
3. We are informed that the U.S. Patent Examiner reviewing our patent application believed that U.S. Patent No. 6,686,820 issued to Qing Ma et al., entitled "MICROELECTROMECHANICAL (MEMS) SWITCHING APPARATUS" (hereinafter "Ma et al.") discloses certain elements of claims 1, 3, 6-9, 12-18, and 21 and anticipates those claims under 35 U.S.C. §102(e), and discloses certain elements of claims 2, 4-5, 10-11, and 19-20 that, in

combination with other references, renders those claims obvious under 35 U.S.C. 103(a), respectively.

4. We conceived every element of claims 1-21 prior to July 11, 2002, which is the filing date of Ma et al.

5. The article entitled "RF MEMS Switches Fabricated on Low Cost Microwave Laminates Using Low Temperature Processes" with dates redacted, attached hereto as Exhibit A, is an accurate reproduction of the original article in our possession.

6. The article entitled "Monolithic Integration of RF MEMS Switches with a Diversity Antenna on PCB Substrate" with dates redacted, attached hereto as Exhibit B, is an accurate reproduction of the original article in our possession.

7. Exhibits A and B disclose, either expressly or inherently, every element of claims 1-21. Exhibits A and B demonstrate that we conceived of every element of claims 1-21 prior to July 11, 2002.

8. We exercised reasonable diligence from the time we conceived of our invention to the time we described our invention to our patent attorney for the purposes of preparing the application to be filed.

9. On information and belief, from the time we described our invention to our patent attorney to the day the provisional patent application 60/437,209 was filed on December 31, 2002, a diligent effort was made in the United States to prepare and review the application. The provisional patent application 60/437,209 discloses all of the elements of claims 1-21 to a degree sufficient for one of ordinary skill in the art to make or use the invention.

10. We further declare that all statements made herein of our own knowledge are true and that all statements made on information and belief are believed to be true; and further that these statements are made with the knowledge that willful false statements and the like so made are punishable by fine or imprisonment, or both, under Title 18, United States Code, § 1001 and that such willful false statements may jeopardize the validity of the application or any patent issuing thereon.

Dated: _____, 2006

Bedri A. Cetiner

Dated: _____, 2006

Mark Bachman

Dated: _____, 2006

Guann-Pyng Li

Dated: _____, 2006

Jiangyuan Qian

Dated: _____, 2006

Hung-Pin Chang

Dated: _____, 2006

Franco De Flaviis

Patent
703427.3

10. We further declare that all statements made herein of our own knowledge are true and that all statements made on information and belief are believed to be true; and further that these statements are made with the knowledge that willful false statements and the like so made are punishable by fine or imprisonment, or both, under Title 18, United States Code, § 1001 and that such willful false statements may jeopardize the validity of the application or any patent issuing thereon.

Dated: January 19, 2006
Bedri A. Cetiner

Dated: _____, 2006

Mark Bachman

Dated: _____, 2006

Guann-Pyng Li

Dated: _____, 2006

Jiangyuan Qian

Dated: _____, 2006

Hung-Pin Chang

Dated: _____, 2006

Franco De Flaviis

10. We further declare that all statements made herein of our own knowledge are true and that all statements made on information and belief are believed to be true; and further that these statements are made with the knowledge that willful false statements and the like so made are punishable by fine or imprisonment, or both, under Title 18, United States Code, § 1001 and that such willful false statements may jeopardize the validity of the application or any patent issuing thereon.

Dated: _____, 2006

Bedri A. Cetiner

Dated: Feb 7, 2006



Mark Bachman

Dated: _____, 2006

Guann-Pyng Li

Dated: _____, 2006

Jiangyuan Qian

Dated: _____, 2006

Hung-Pin Chang

Dated: _____, 2006

Franco De Flaviis

10. We further declare that all statements made herein of our own knowledge are true and that all statements made on information and belief are believed to be true; and further that these statements are made with the knowledge that willful false statements and the like so made are punishable by fine or imprisonment, or both, under Title 18, United States Code, § 1001 and that such willful false statements may jeopardize the validity of the application or any patent issuing thereon.

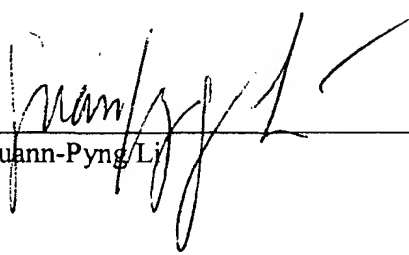
Dated: _____, 2006

Bedri A. Cetiner

Dated: _____, 2006

Mark Bachman

Dated: Feb. 7, 2006



Guann-Pyng Li

Dated: _____, 2006

Jiangyuan Qian

Dated: _____, 2006

Hung-Pin Chang

Dated: _____, 2006

Franco De Flaviis

Patent
703427.3

10. We further declare that all statements made herein of our own knowledge are true and that all statements made on information and belief are believed to be true; and further that these statements are made with the knowledge that willful false statements and the like so made are punishable by fine or imprisonment, or both, under Title 18, United States Code, § 1001 and that such willful false statements may jeopardize the validity of the application or any patent issuing thereon.

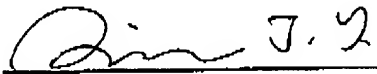
Dated: _____, 2006

Bedri A. Cetiner

Dated: _____, 2006

Mark Bachman

Dated: _____, 2006

Guann-Pyng LiDated: Jan. 23, 2006
Jiangyuan Qian

Dated: _____, 2006

Hung-Pin Chang

Dated: _____, 2006

Franco De Flaviis

10. We further declare that all statements made herein of our own knowledge are true and that all statements made on information and belief are believed to be true; and further that these statements are made with the knowledge that willful false statements and the like so made are punishable by fine or imprisonment, or both, under Title 18, United States Code, § 1001 and that such willful false statements may jeopardize the validity of the application or any patent issuing thereon.

Dated: _____, 2006

Bedri A. Cetiner

Dated: _____, 2006

Mark Bachman

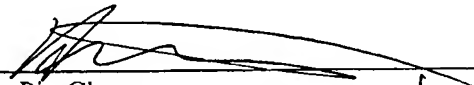
Dated: _____, 2006

Guann-Pyng Li

Dated: _____, 2006

Jiangyuan Qian

Dated: 02/08, 2006



Hung-Pin Chang

Dated: _____, 2006

Franco De Flaviis

10. We further declare that all statements made herein of our own knowledge are true and that all statements made on information and belief are believed to be true; and further that these statements are made with the knowledge that willful false statements and the like so made are punishable by fine or imprisonment, or both, under Title 18, United States Code, § 1001 and that such willful false statements may jeopardize the validity of the application or any patent issuing thereon.

Dated: _____, 2006

Bedri A. Cetiner

Dated: _____, 2006

Mark Bachman

Dated: _____, 2006

Guann-Pyng Li

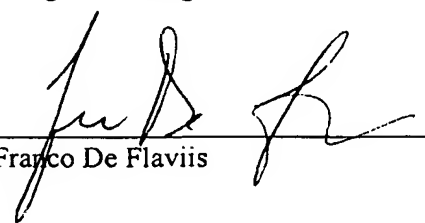
Dated: _____, 2006

Jiangyuan Qian

Dated: _____, 2006

Hung-Pin Chang

Dated: FEB - 8, 2006



Franco De Flaviis

EXHIBIT A

RF MEMS Switches Fabricated on Low Cost Microwave Laminates Using Low Temperature Processes

B. A. Cetiner, *Member, IEEE*, H. P. Chang, J. Y. Qian, *Student Member, IEEE*, M. Bachman,
G. P. Li, *Member, IEEE* and F. De Flaviis, *Member, IEEE*

Abstract—This paper reports RF MEMS switches fabricated on microwave laminate printed circuit boards (PCBs) by using low temperature fabrication processes. The work is novel in that RF MEMS switches can be fabricated on to PCBs and the way they are fabricated. The novel fabrication process, low temperature (90-170°C) high density inductively coupled plasma chemical vapor deposition (HDICP CVD) is the key process allowing substrate-independent MEMS technology while at the same time providing higher performance, yield, and reliability. The fabrication steps are described in detail and the characterization of switches is provided. This technology allows the choice of any substrate with desired electrical properties for antenna applications such as RT/duroid5880 ($\epsilon_r=2.2$, $\tan\delta=0.0004$) and integration RF MEMS switches with antenna elements. As a proof of concept a multi-element antenna system integrated with RF MEMS switches is designed and fabricated. Results are presented and discussed.

Index Terms—RF MEMS switches, low temperature process, printed circuit board.

I. INTRODUCTION

RF MEMS is a new emerging sub area of MEMS technology that is revolutionizing and making a big impact to today's RF and microwave applications. Its low power, high performance, tuning range, and integration capability are the key characteristics enabling potential improvements in size, cost, and increased functionality. It is also a potential technology of choice holding a strong promise to meet the performance expectations of next generation communication systems.

RF MEMS switches are the basic building blocks to the RF MEMS circuits. These switches have been demonstrated to have outstanding RF performance, very low insertion loss and high isolation [1], [2]. In addition, they are ultra low power devices and have very linear behavior with extremely low signal distortion [3]. Such features make them very attractive

for modern radar and communications applications. RF MEMS circuits such as variable capacitors, filters, on-chip inductors, and phase shifters with RF MEMS switches as building blocks have demonstrated superiority over existing circuits [4], [5], [6], [7].

Although emphasis has largely been focused on and well established for RF performance of these switches, many efforts are still needed for state of the art RF MEMS switches in order to establish and improve their reliability while at the same time providing higher yield and reproducible performance. While the manufacturing cost is very low, the cost of a packaged RF MEMS switch component is much higher than its semiconductor counterparts (FET, pin-diode) since packaging is still a major cost driver in current MEMS technology.

We believe a system level approach to current MEMS technology involving the development of novel fabrication processes is the key to providing cost reduction as a consequence of functionality enhancement. With this motivation, specifically addressed in this paper is a novel fabrication process, low temperature high density inductively coupled plasma chemical vapor deposition (HDICP CVD), with emphasis on its use in achieving substrate-independent RF MEMS technology with higher yield and reliability. The HDICP CVD process is described and the resulting SiN_x layer is characterized in section II of this paper.

Cost take-out is mainly being achieved by using a HDICP CVD process that enables building RF MEMS switches on a very low-cost microwave laminate PCBs such as RO4003-FR4 substrate ($\epsilon_r=3.38$, $\tan\delta=0.002$) [8] eliminating the necessity of expensive semiconductor substrates such as gallium arsenide, high-resistivity silicon, or alumina. The wide spread use of PCB technologies in the majority of today's wireless systems has also motivated us to develop RF MEMS technology compatible to very well established industry standard PCB technology. The other factor that reduces overall system cost is the elimination of some of the processing steps involved in typical RF MEMS switch fabrication owing to the compatibility between PCB and the proposed RF MEMS technologies. The fabrication process steps for reconstructing RF MEMS switches on a RO4003-FR4 substrate are given in section III. The topology of the RF MEMS switches here presented is similar to the one described in [1].

Manuscript received [redacted]. This work was supported in part by DARPA under Grant No. MDA 97201-1-0025.

The authors are with the Electrical Engineering and Computer Science Department, The University of California at Irvine, Irvine, CA 92617, USA (telephone: 949-824-6181, e-mail: bedri@uci.edu, qianj@uci.edu, hungpinc@uci.edu).

In addition to improvement in cost, the developed technology allows capability of MEMS integration with PCB components that enhance the functionality of the system. In section IV, as a proof of concept we carried out the design and fabrication of a MEMS integrated antenna system fabricated on a PCB. The structure of antenna elements and RF MEMS switches allow monolithic batch fabrication by eliminating hybrid assembly, which is critical to lowering cost.

Another important impact of this technology is on multichip module (MCM) technology. The needs for enhancing the functionality, efficiency, and reliability with simultaneous cost reduction in microwave and millimeter-wave applications have triggered much interest in the development of novel multilayer packaging and interconnect technologies. Consequently there have been fundamental advances in (MCMs) with high-density integration [9]. More recently silicon micromachined circuit integration, which also shows exceptional promises for MEMS integration and packaging, has been offered to overcome some of the drawbacks of MCM technology such as high losses of interconnects and passive components [10], [11]. Typical MCM structure consists of multiple MMICs, transmission lines established on different dielectric layers, vertical interconnects, and feedthroughs, all encapsulated in a package. A number of MCMs are solder attached on to a PCB to form a very high-density microwave or millimeter-wave sub system. As a result of this high-density environment, the losses of the interconnects and coupling between circuits are inevitable and severely degrade the overall system performance. The developed RF MEMS technology, however, allows establishing MEMS circuitry directly on PCB eliminating some of the interconnect losses between MCM and PCB. This results in improvement in overall system performance and lower cost.

II. LOW TEMPERATURE HDICP CVD PROCESS

Plasma enhanced chemical vapor deposition (PECVD) is the most common method of depositing silicon nitride (SiN_x) film in today's RF MEMS switch fabrication. If one, however, considers the fact that a typical maximum operating temperature of many of the PCBs is approximately 150°C , PECVD with $250\text{--}400^\circ\text{C}$ process temperatures cannot be employed for these substrates.

A novel process method, a very low-temperature ($90\text{--}170^\circ\text{C}$) HDICP CVD to deposit SiN_x film has recently been developed at the University of California, Irvine, Integrated Nanosystems Research Facility (UCI INRF) [12]. Results showed that SiN_x film deposited using the HDICP CVD method has excellent

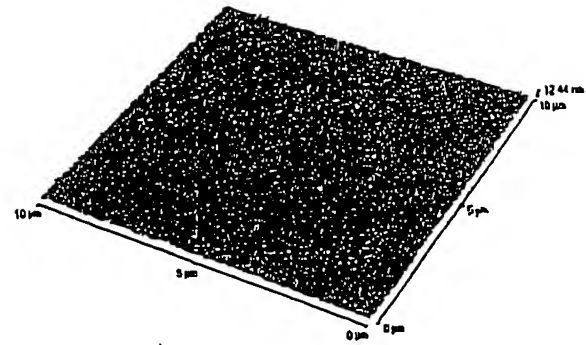


Fig.1 AFM micrograph of the 500W, 90°C SiN_x surface

film properties and offers advantages in RF MEMS switch technology over the SiN_x films deposited by conventional PECVD. HDICP CVD SiN_x has higher breakdown voltage, less pinhole density, and better uniformity than PECVD SiN_x .

The HDICP CVD method uses inductively coupled RF power to create high-density plasma in the processing reactor. The power from a RF generator is inductively coupled into the plasma chamber through a strategically located and designed antenna array. A set of magnets with Faraday shield copper tapes wrapped around them is also utilized to further enhance the plasma density and to adjust the plasma profile. As a result, HDICP CVD plasma density can be as high as $10^{10}\text{--}10^{11}$ ions/ cm^3 , whereas a typical PECVD plasma density is approximately 10^9 ions/ cm^3 . It is this high-density plasma that allows deposition to take place at very low temperatures. A plasma profile with an excellent uniformity is this method's distinct feature that allows depositing very thin films with smooth surface across the wafer. A plasma density varying across the chamber results in different deposition rates within the wafer and causes poor uniformity for the deposited SiN_x films. The irregularities in the profile of the SiN_x film make accurate control of down state capacitance difficult and create a big challenge for a distributed phase shifter described in [6]. On the other hand, HDICP CVD SiN_x with perfect uniformity can easily provide excellent control of down position capacitance resulting in better reliability of the device.

Firstly, we performed an atomic force microscopy (AFM) measurement to obtain the root-mean-square (RMS) roughness of HDICP CVD nitride films, and compared them to those deposited by PECVD. SiN_x films of $0.1\mu\text{m}$ thickness are deposited on top of the Cu layer, as in the RF MEMS switch device, using three different operation conditions for HDICP CVD and an optimum condition for PECVD. Results are given

TABLE I: COMPARISON OF RMS ROUGHNESS (μm) BETWEEN HDICP CVD AND PECVD SiN_x FILMS.

HDICP CVD			PECVD	
500W, 90°C	500W, 170°C	800W, 170°C	250°C	300°C [1]
1.6	2.0	2.2	2.5	3.1

in Table I and indicate that the SiN_x films deposited at lower temperatures possess smaller RMS values. It should be noted herein that the low temperature nature of HDICP CVD method prevents the Cu electrode, on which SiN_x is deposited, from being exposed to high temperatures that may cause hillocking problems. If PECVD process is used to deposit the nitride layer, this hillocking problem is inevitable and needs to be limited by depositing another layer of metal with a high melting temperature on top of the Cu electrode [1]. This extra process step, however, is not desirable for achieving simplicity of the fabrication procedure. The roughness of SiN_x film has significant influence on the switch down state capacitance, C_{down} . The smooth surface of the nitride film provides intimate contact with the metal membrane of the RF MEMS switch so that the contact area is increased providing higher down state capacitance, which is critical in order to achieve desired capacitance ratio for better switching performance. The capacitance ratio is given by,

$$\frac{C_{down}}{C_{up}} = \frac{\epsilon_r t_{air} + t_{diel}}{t_{diel}} \quad (1)$$

where C_{up} represents the up state capacitance, t_{air} is the thickness of the air layer from top of the nitride film to the bottom of the membrane, t_{diel} and ϵ_r are the thickness and the dielectric permittivity of the SiN_x layer, respectively. Fig.1 shows the AFM measurement image of SiN_x film surface deposited by HDICP CVD at the conditions of 90°C and 500W that exhibited smoothest surface.

To obtain the dielectric strength of the nitride film, we used metal-insulator-semiconductor (MIS) structure, in which SiN_x film is sandwiched between the Cu contact and Si substrate. Current density-electric field (J-E) measurements were carried out with the HP 4145B parameter analyzer. Fig.2 shows the J-E curves for 0.1μm SiN_x films deposited by HDICP CVD and PECVD methods. The observed breakdown strengths of the three HDICP CVD SiN_x films are larger than 9 MV/cm.

The other advantage of the HDICP CVD method over the PECVD method is its capability of depositing SiN_x films as

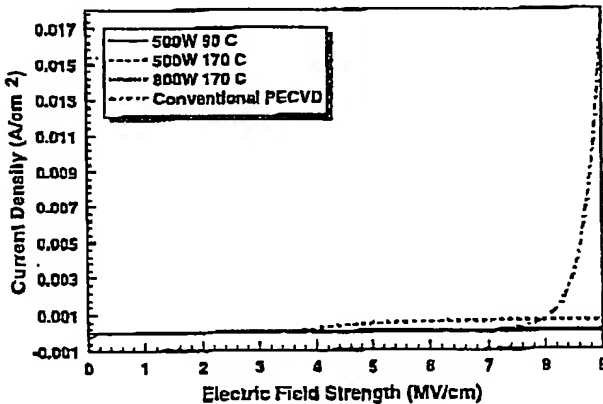


Fig. 2 J-E characteristics of HDICP CVD and PECVD SiN_x films

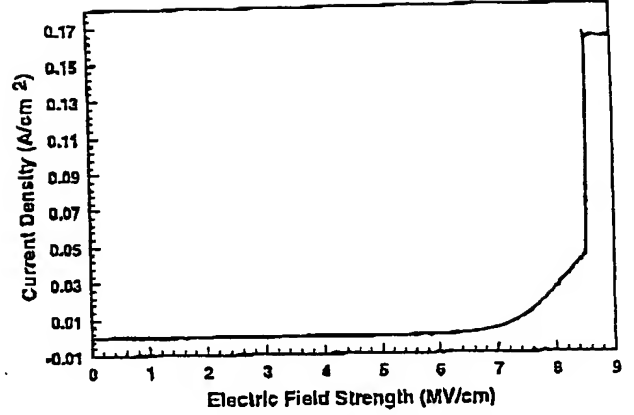


Fig. 3: J-E curves of the HDICP CVD SiN_x film of 250 Å.

thin as 250Å. According to equation (1), a thinner SiN_x film results in a higher capacitance ratio. However, as indicated by Muldavin, et al [2], it is impractical to deposit PECVD SiN_x films thinner than 1000Å due to a large pinhole density that results in low dielectric breakdown strength. We used 250Å thick SiN_x film deposited by HDICP CVD at the operating conditions of 800W and 90°C to determine its breakdown voltage. As seen in Fig.3 breakdown voltage is around 9 MV/cm. This result proves that SiN_x films as thin as 250Å can be used in RF MEMS switch devices withstanding typical actuation voltage (20-50V) without dielectric breakdown. RF MEMS switches fabricated with HDICP CVD process demonstrated a dramatic increase in their down position capacitance, providing better switching performance and an additional degree of freedom in RF MEMS switch design [12]

III. FABRICATION PROCESS AND CHARACTERIZATION

A. Fabrication

An important advantage of the fabrication technology described in this paper is its compatibility with industry standard PCB technology, thus reducing the total process steps involved in typical RF MEMS switch fabrication. This fabrication technology is substrate independent and offers versatility in substrate selection from microwave laminate substrate families. We opted for the RO4003-FR4 [8] high performance laminate ($\epsilon_r=3.38$, $\tan\delta=0.002$) since it is a preferred PCB for wireless applications due to its very low cost and capability to handle the required higher frequencies.

The fabrication begins with RO4003 laminate with copper layers of 8.5μm on both sides. The dielectric thickness is 1.57mm. The fabrication procedure is relatively simple and requires only 4 masks. Fig.4 shows the brief fabrication sequence. As a first step, etching the copper layer down on one side and removing the one on the other side forms CPW lines. For 50ohm CPW line the width of the center conductor and that of the gap separating ground plane from center conductor are chosen to be 180μm and 40μm, respectively. Next, a thin layer of HDICP CVD SiN_x is deposited at the operating condition of 500W RF power and 90°C temperature.

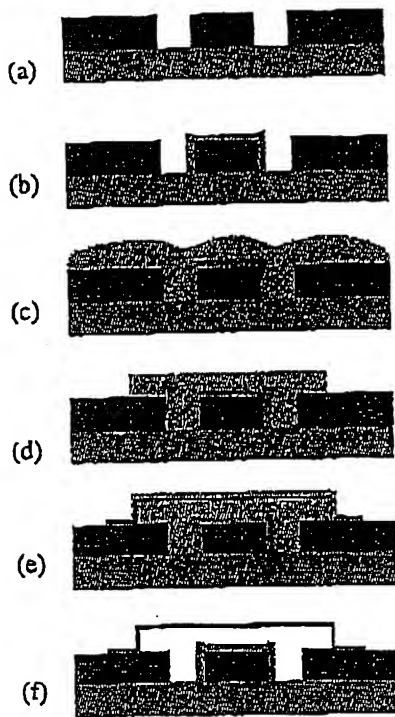


Fig. 4 Process flow of RF MEMS switches fabricated on microwave laminate substrates. (a) Cu etching: Antennas and all planar parts of the system are fabricated at this step. (b) deposition of HDICP CVD SiNx. (c) Deposition of sacrificial photoresist layer. (d) CMP process. (e) Deposition of Al alloy membrane metal. (f) Removing sacrificial photoresist layer to release the membrane

Following SiNx deposition, the film is etched by reactive ion etching (RIE) such that it only insulates the central portion of the CPW signal line providing capacitive contact between signal line and ground plane for the switch down state. Next, a sacrificial photoresist layer needs to be applied over the surface consisting of different heights, due to CPW lines with metal thickness of $8.5\mu\text{m}$. This is the critical processing step, since it is difficult to apply a uniform coat of photoresist on a surface with different heights. On the other hand, one of the keys to success in obtaining mechanically reliable membrane structure lies in obtaining a very uniform profile in the patterned sacrificial photoresist layer on which the metal membrane is deposited. To overcome this difficulty we use a planarization technique developed at the UCI INRF [13]. This technique is called compressing molding planarization and is

briefly described as follows: The photoresist is first applied by spin coating with low spinning speed to create a photoresist layer with a much higher thickness than that of metal in the CPW lines. It is then partially soft baked to drive off the solvent inside. Next, a mold master is applied on top of the photoresist film for molding. The mold material is carefully chosen based on the properties of the film material to prevent the photoresist film from sticking to it during the process. We use AZ 4600 photoresist as a sacrificial layer, and polydimethylsiloxane (PDMS) is chosen as the mold material. The PDMS coated mold is then capped on the photoresist layer by a presser. During the molding process heat is also applied to the presser to soften and mold the photoresist layer. The spacer with a specific thickness used to stop the molding process defines the desired thickness for the sacrificial layer. The thickness of this sacrificial layer determines the height of the membrane over the CPW line, here chosen to be $5\mu\text{m}$. After the molding process, the substrate is cooled down and released from the PDMS mold. Fig.5 shows the film profiles of the sacrificial photoresist layer obtained by using the tencor alpha step with and without CMP process. It is evident that the CMP process is capable of providing a very flat surface with precise control of film thickness. Following the CMP process, the sacrificial photoresist layer is patterned into the required membrane pattern. We then use low temperature metal sputtering process to deposit an Al alloy membrane layer of $0.5\mu\text{m}$ thickness followed by selective wet etching. It is worth noting that this low temperature sputtering process not only satisfies the compatibility requirement with the substrate independent MEMS technology, but also reduces compressive stress and eliminates stress gradients that occur in thin (less than $1\mu\text{m}$) metal films. A commonly used technique to control thin film stress is annealing but it requires very high temperatures ($300\text{--}900^\circ\text{C}$) that make it incompatible with MEMS fabrication on PCBs. The last process step is to remove the sacrificial PR layer by soaking the wafer in acetone to release the membranes. After removing the wafer from acetone, it is rinsed in boiling methanol to eliminate liquid surface tension of the membranes in order to prevent them from being pulled down on SiNx film [14]. This last step combined with CMP and low temperature sputtering techniques play a significant role on membrane release yield. Indeed, our release yield is almost 100%.

B. Measurements

The RF characterization of the MEMS switches was done using a HP 8510C network analyzer connected to a Cascade probe station. The system was calibrated using standard thru-reflection-line (TRL) on-wafer standards. S-parameter data was recorded over the frequency range of $0.1\text{--}20\text{GHz}$, according to the frequency specifications given for RO4003-FR4 [8].

The measured insertion loss and return loss of the switch in the up state is illustrated in Fig.6a. The switch has approximately 0.1dB loss at 10GHz and 0.35dB at 20GHz . The insertion loss of this switch is slightly higher compared to

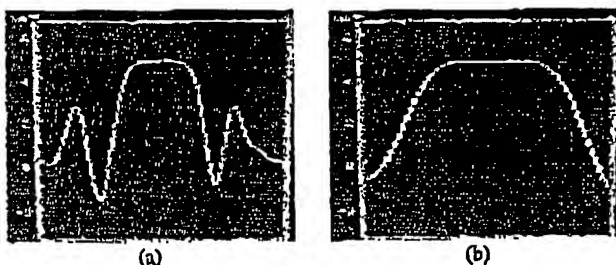


Fig. 5 Film profiles of the sacrificial photoresist layers (a) without CMP process (b) with CMP process

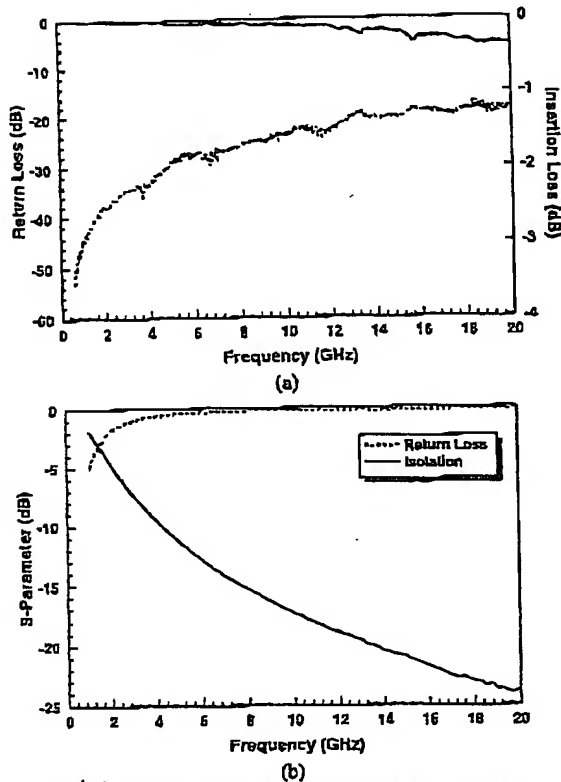


Fig. 6 Measured S-parameters for the RF MEMS switches fabricated on RO4003-FR4 in (a) the up position and (b) the down position

those of typical RF MEMS switches fabricated on semiconductor substrates. This is due to the dielectric losses of the substrate in addition to the ohmic losses of copper metal. To carry out the down position RF measurements, we used external bias-tee circuits and the bias voltage was set at 30V, which is found to be the typical pull down voltage for these switches. The results are shown in Fig.6b. The isolation is about 18dB at 10GHz and 24dB at 20GHz.

IV. PROOF OF CONCEPT: MEMS SWITCHED ANTENNA

A MEMS switched antenna was designed and built on a microwave laminate PCB substrate to establish a proof of concept for the developed RF MEMS technology. We used RT/duroid 5880 microwave laminate [8] since it offers better performance for antenna applications owing to its very low

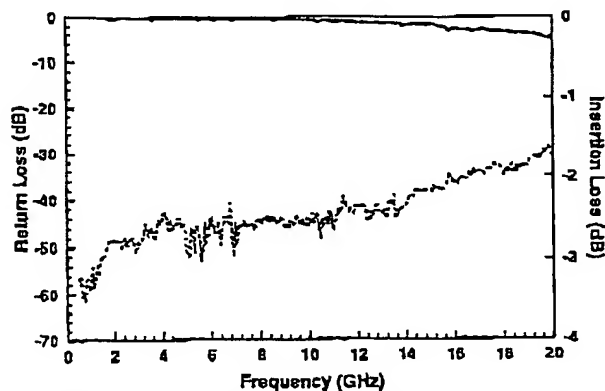


Fig. 7 Measured S-parameter for the RF MEMS switches fabricated on RT/duroid 5880

loss property ($\epsilon_r=2.2$, $\tan\delta=0.0004$). We designed, fabricated, and measured individual switches and antennas at first.

The measured s-parameters for the RF MEMS switches

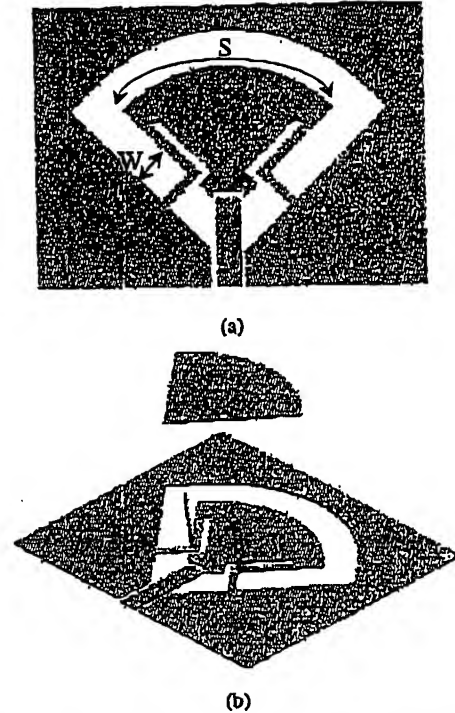


Fig. 8 Schematic of antenna geometry (a) Top view of the bottom layer, $W=2\text{mm}$, $S=15\text{mm}$ (b) 3-dimensional schematic

fabricated on RT/duroid 5880 are shown in Fig.7. Parallel to the lower loss characteristics of duroid material, the RF performance is better than of those fabricated on RO4003 substrate. The insertion loss is about 0.05dB at 10GHz and 0.2dB at 20GHz.

The antenna structure used in this integrated system has evolved from the previously introduced so-called q-dime antenna structure [15]. In order to create an antenna structure that is compatible with PCB technology and suitable to MEMS integration, the structure of the q-dime antenna with three-metalization layers is modified such that an antenna structure with two metalization layers is obtained. In addition, this antenna structure is fed by a CPW line as opposed to the coax

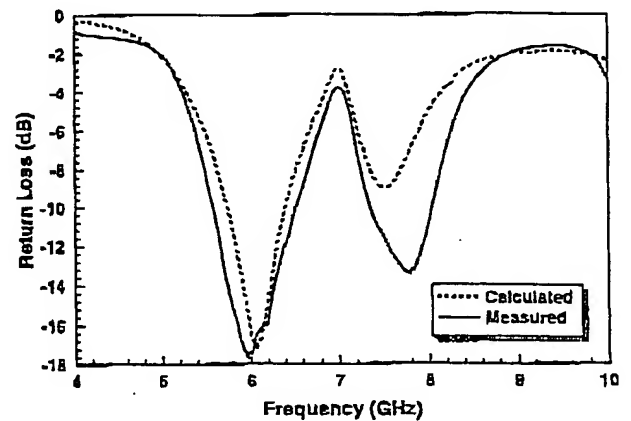


Fig. 9 Measured and calculated return loss of the antenna

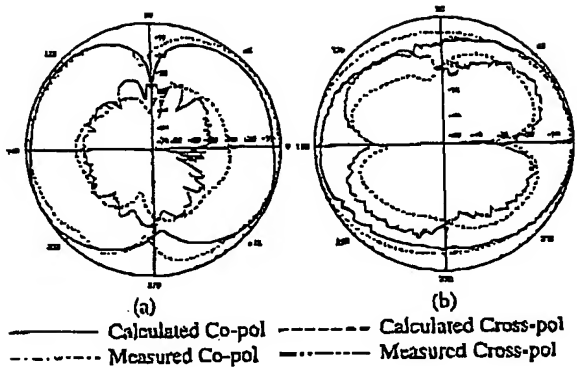


Fig. 10 Measured and calculated radiation pattern of the antenna at 6GHz (a) in E-plane (x-z plane) (b) in H plane (y-z plane)

feed of the q-dime allowing easier integration with CPW RF MEMS switches. The schematic of the antenna geometry is shown in Fig.8. Vertical and horizontal slots radiate the electromagnetic field from this antenna. The vertical slot is formed between two sectoral patches, namely top and bottom patches, formed on top and bottom metalization layers of the RT/5880 duroid laminate. The bottom layer of the structure is connected to the upper layer through symmetric vertical walls with thickness of 1.57mm. The bottom layer contains the bottom patch, CPW feed line, and the horizontal slot (see Fig.8a). The measured and calculated impedance characteristic of the antenna is shown in Fig.9. The antenna possesses dual band behavior due to the two-slot structure. For a 1:2 VSWR, 15% bandwidth is achieved for the first frequency band. If it is desired, broader bandwidth for single band operation can be obtained by optimizing antenna dimensions. Fig.10a and Fig.10b show the co-polar and cross-polar measured radiation patterns of the antenna in x-z and y-z planes, respectively. In accordance with its geometry and size, the antenna exhibits co-polar orientation parallel to the field orientation existing on the slots, E_θ on the x-z plane and E_ϕ on the y-z plane.

The fabrication of the MEMS switched antenna starts with building its planar parts. These include top and bottom layer of the antenna structure, CPW lines for switches, dc bias and dc block circuits. Two masks containing the definitions of these planar geometries are used for the process step of Cu etching. Next we use vias with 0.2mm diameter to connect bottom and top metal layers. After obtaining this structure we continue to

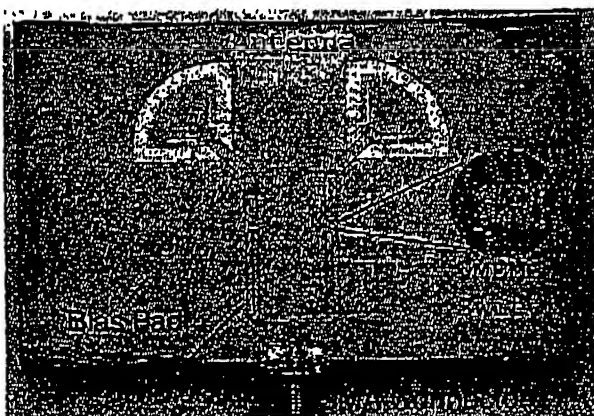


Fig. 11 Photograph of the MEMS-Switched-Antenna System

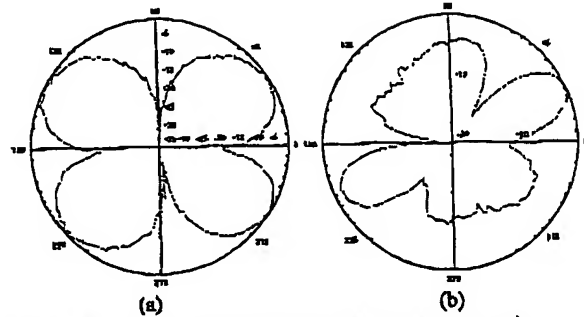


Fig. 12 Measured radiation pattern of the MEMS-Switched-Antenna system at 6GHz in y-z plane (a) H-pol (b) V-pol

fabricate RF MEMS switches as explained in section III.

Fig.11 shows the fabricated MEMS-switched antenna system. The system consists of two antenna elements and two RF MEMS switches located on CPW feed lines to guide the RF signal between two antennas. RF MEMS switches enable to activate either antenna element for spatial or angular diversity, or operate them together to create a superposition radiation pattern for coverage reconfigurability. Antennas are placed at 90° , so that by operating either antenna, orthogonal radiation patterns are obtained. We used high RF impedance quarter wavelength lines for dc bias voltage to prevent RF signal from being shorted by the power supply. Similarly, quarter wavelength dc block circuits isolate the dc bias signal from microwave signal (see Fig.11). These quarter-wavelength dc block circuits are from the RF MEMS switches to the output ports of the tee junction. These lines translate the RF short at the RF MEMS switch locations to an RF open at the output ports of the tee junction. In other words, when either of the switches is actuated, RF signal sees an open at the output port of the tee junction on the actuated switch side so that RF signal can be directed to either path to sequentially operate the antennas. Fig.12a and Fig.12b illustrate the measured y-z plane V-pol and H-pol radiation patterns corresponding to the simultaneous operation of both antennas. Switching between antenna elements generates different spatial radiation patterns that can be employed for spatial or angular diversity techniques [16] to increase receiver performance of the communication system.

V. CONCLUSIONS

Substrate-independent RF MEMS technology featuring novel low temperature fabrication processes are developed in this work. Particular emphasis is given to microwave laminate PCB substrates due to their low cost and widespread use in wireless communication systems. This technology allows construction of RF MEMS switches on PCB substrates and thus provides enhanced overall system performance and functionality for high-density microwave subsystems consisting of multichip modules (MCMs). High-performance substrates with desired electrical properties for MEMS integrated antenna systems can be chosen for high system efficiency. Present and future communication systems are likely to benefit from this MEMS technology in terms of its

reliability, high yield, low cost, and increased system functionality.

ACKNOWLEDGMENT

The authors would like to thank Prof. N.G. Alexopoulos for helpful discussions and comments on the antenna system. We are grateful for Dr. Q. Xu and J. H. T. Lin for their helps in the process.

REFERENCES

- [1] Z.J. Yao, S. Chen, S. Eshelman, D. Denniston and C. Goldsmith, "Micromachined low-loss microwave switches," *IEEE Journal of Microelectromechanical Systems*, vol. 8, no. 2, pp. 129-134, June 1999.
- [2] J. B. Muldavin and G. M. Rebeiz, "High-isolation CPW MEMS shunt switches: Modeling and Design," *IEEE Trans. Microwave Theory and Tech.*, vol. MTT-48, no. 6, pp. 1045-1056, June 2000.
- [3] F. De Flaviis, R. Coccioli, and T. Itoh, "Non linear analysis and evaluation of distortion introduced by MEM switches in reconfigurable antenna systems," *IEEE AP-S Int. Symp.*, Davos, Switzerland, 2000.
- [4] N. S. Barker and G.M.Rebeiz, "Distributed MEMS true-time delay phase shifters and wide-band switches," *IEEE Trans. Microwave Theory and Tech.*, vol. MTT-46, no.11, pp. 1881-1890, November 1998.
- [5] C.L.Goldsmith, A.Malczewski, Z.J.Yao, C.Shea, J.Ehmke, and D.H.Hinzel, "RF MEMS variable capacitors for tunable filters," *Int. J. of RF and Microwave Computer-Aided Eng.*, vol.9, no.4, pp.362-374, July 1999.
- [6] A. Borgioli, Y. Liu, A.S. Nagra, and R.A. York, "Low-loss distributed MEMS phase shifter," *IEEE Microwave Guided Wave Lett.*, vol. 10, no. 1, pp. 7-9, January 2000.
- [7] E.R. Brown, "RF-MEMS switches for reconfigurable integrated circuits," *IEEE Trans. Microwave Theory and Tech.*, vol. MTT-46, no.11, pp. 1868-1880, November 1998.
- [8] Rogers Inc. Microwave Products Technical Information, 2001.
- [9] A.H. Pham, A. Sutono, J. Laskar, V. Krishnamurthy, D. Lester, E. Balch, and J. Rose, "Development of microwave multiplayer plastic-based multichip modules," *IEEE Trans. Advanced Packaging.*, vol. 24, no. 1, pp. 37-40, February 2001.
- [10] R.M. Henderson, and L.P.B. Katchi, "Silicon-based micromachined packages for high-frequency applications," *IEEE Trans. Microwave Theory and Tech.*, vol. MTT-47, no.8, pp. 1563-1569, August 1999.
- [11] A. Murgomenos, D. Peroulis, J. P. Becker, and L.P.B. Katchi, "Silicon micromachined interconnects for on-wafer packaging of MEMS devices," *2001 IEEE Topical Meeting on Silicon Monolithic Integrated Circuits in RF Systems*, pp.33-36, September 2001.
- [12] C.H. Chang, J.Y. Qian, B. A. Cetiner, Q. Xu, M. Bachman, F. De Flaviis, and G.P. Li, "RF MEMS capacitive switches fabricated with HDICP CVD SiN_x," *2002 IEEE MTT-S Int. Microwave Symp.*, June 2002, to be presented.
- [13] H.P. Chang, J.Y. Qian, M. Bachman, P. Congdon, and G.P. Li, "A novel technique for fabrication of multi-layered micro coils in microelectromechanical system applications", *2002 SPIE Int. Symp. On Smart Structures and Materials.*, March 2002.
- [14] A. Takashi, W.C. Messner, and M.L. Reed, "Effects of elevated temperature treatments in microstructure release procedures," *IEEE Journal of Microelectromechanical Systems*, vol. 4, no.2, pp. 66-75, June 1995.
- [15] L. Jofre, B.A.Cetiner, and F. De Flaviis, "Miniature Multielement Antenna for Wireless Communications", *IEEE Trans. on Antennas and Propagation Special Issue on Wireless Communications*, to be published.
- [16] R.R Ramirez and F. De Flaviis, "A mutual coupling study of linear polarized microstrip antennas for diversity wireless systems", *IEEE Trans. on Antennas and Propagation*, to be published.

EXHIBIT B

Monolithic Integration of RF MEMS Switches With a Diversity Antenna on PCB Substrate

B. A. Cetiner, *Member, IEEE*, J. Y. Qian, H. P. Chang, M. Bachman, G. P. Li, and F. De Flaviis

Abstract—A novel process for monolithic integration of RF microelectromechanical system (MEMS) switches with three-dimensional antenna elements on a microwave laminate printed circuit board (PCB) is presented. This process calls for a low-temperature (90°C – 170°C) high-density inductively coupled plasma chemical vapor deposition technique that allows the choice of any PCB substrate, such as RO4003-FR4 ($\epsilon_r = 3.38$, $\tan \delta = 0.002$), with the desired electrical properties for antenna applications. A two-element diversity antenna system monolithically integrated with RF MEMS switches is designed and demonstrated.

Index Terms—RF microelectromechanical system (MEMS) switches, monolithic integration, low-temperature process, printed circuit board (PCB).

I. INTRODUCTION

RF microelectromechanical system (MEMS) technology is an emerging subarea of MEMS technology that is revolutionizing RF and microwave applications. RF MEMS switches are basic building blocks for a variety of new RF MEMS circuits. These switches have demonstrated outstanding RF performance, very low insertion loss, and high isolation [1], [2]. In addition, they operate at ultra-low power levels with excellent linearity and extremely low signal distortion. Such features make them very attractive for modern radar and communications applications. RF MEMS circuits such as variable capacitors and phase shifters built upon RF MEMS switches have demonstrated superiority over existing ones [3], [4].

While the manufacturing cost of a single die is very low due to batch processing, a packaged RF MEMS switch component is expensive compared to its semiconductor counterparts (i.e., FETs, p-i-n diodes). This is because packaging is still a major cost driver in current MEMS technology. We believe developing novel integrated-system fabrication processes through a system-level approach is key to reducing the cost of RF MEMS as a result of functionality enhancement. This can be achieved by integrating RF MEMS switches with other circuit elements. For example, monolithic integration of RF MEMS switches with power amplifiers on a GaAs substrate has been demonstrated [5]. Batch transfer integration and flip-chip assembly to place MEMS on different substrates have been proposed [6], [7]. More recently, integration of two-dimensional antenna

elements with RF MEMS switches on a glass substrate was also presented [8]. While the RF MEMS switch systems have been demonstrated in these papers, they are still limited in RF performance due to the substrate materials used for construction, or limited in production cost due to the nonbatch process. In order to alleviate such substrate constraints and to facilitate three-dimensional (3-D) design that exploits performance limits of small size antennas [9], it is worthwhile exploring an alternative integrated system technology to address system application needs and to optimize system performance.

In this paper, we describe the monolithic integration of 3-D antenna structures with RF MEMS switches on a printed circuit board (PCB) to construct a diversity antenna. The compatible structures of an antenna element and RF MEMS switch allow monolithic batch fabrication, thus eliminating hybrid assembly. Low production cost is expected in this process by building the integrated RF MEMS-switched antenna directly on a low-cost microwave laminate PCB without requiring packaging individual components and matching impedance among various RF components. To demonstrate the integration concept on a PCB, we have chosen an RF MEMS-switched antenna that can be employed in diversity techniques and radiation pattern reconfigurability to improve receiver performance. The system is physically compact so that it can be integrated easily with portable communication devices.

II. ANTENNA, RF MEMS SWITCH, AND THEIR INTEGRATION

A. RF MEMS Switch

In this research, RO4003-FR4 [10] was used as a substrate due to its low cost and widespread use in wireless systems. We note that any PCB substrate such as RT/Duroid5880 ($\epsilon_r = 2.2$, $\tan \delta = 0.0004$) can also be used depending on the intended application. The topology of the RF MEMS switches used here is similar to the one described in [1]. The fabrication procedure¹ requires only three masks [11] due to its compatibility with PCB technology. The SiN_x layer providing capacitive contact at the switch down position is deposited by using a novel low temperature (90°C – 170°C) high-density inductively coupled plasma chemical vapor deposition (HDICP CVD) instead of conventional PECVD. PECVD with 250°C – 400°C process temperatures cannot be employed for many of the PCBs, which have typical operating temperatures of 150°C – 200°C . In addition to its low-temperature nature, HDICP CVD SiN_x has higher breakdown voltage, less pinhole density, and better uniformity than PECVD SiN_x [12]. A brief fabrication sequence

Manuscript received [redacted]; revised [redacted]. This work was supported in part by the Defense Advanced Research Projects Agency under Grant MDA 97201-1-0025.

The authors are with the Electrical Engineering and Computer Science Department, The University of California at Irvine, Irvine, CA 92617 USA (e-mail: bedri@uci.edu).

Digital Object Identifier 10.1109/TMTT.2002.806521

¹Patent pending, UC Case 2002-369-1.

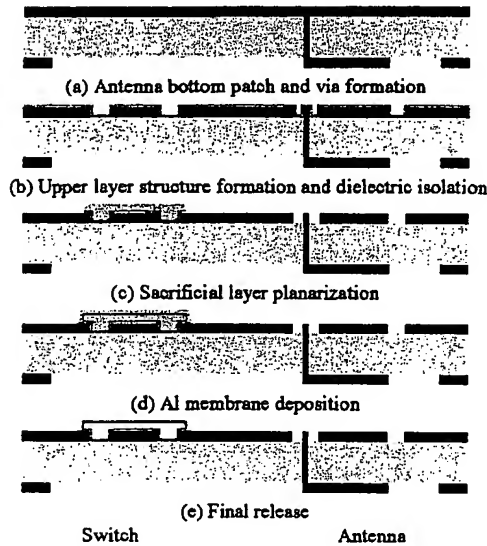


Fig. 1. Process flow of monolithically fabricated RF MEMS switched diversity antenna on RO4003-FR4 PCB.

(see Fig. 1) for the RF MEMS switch is given as the construction of the integrated antenna is described in Section II-C. Measured s -parameters of switches fabricated on RO4003-FR4 PCB showed excellent RF characteristics similar to those of switches fabricated on semiconductor substrates [11].

B. Antenna Element

The antenna structure used in this integrated system has evolved from the q -dime antenna structure [9]. In order to achieve compatibility with PCB technology and MEMS monolithic integration, we modify the q -dime antenna structure to contain only two metallization layers. In addition, this antenna structure is capacitively fed by a coplanar waveguide (CPW) line, as opposed to the coax feed of the q -dime. This allows easier integration with CPW RF MEMS switches. The schematic of the antenna geometry is shown in Fig. 2 (The bottom patch is shown as separated, in Fig. 2(b), for the sake of the illustration.) Vertical and horizontal slots radiate the electromagnetic energy from this antenna. The vertical slot is formed between two sectoral patches, namely, the upper and bottom patches, formed on the upper and bottom metallization layers, respectively, of the RO4003-FR4 laminate with copper layers of $16.5 \mu\text{m}$ and a dielectric thickness of 1.57 mm . The bottom layer of the structure is connected to the upper layer by two vertical walls. The upper layer contains the upper patch, CPW feed line, and the horizontal slot [see Fig. 2(a)].

C. RF MEMS Switch Integrated Antenna and Measurements

The fabrication of the MEMS-switched antenna starts with building its bottom layer (bottom patches) and vias to connect the bottom layer of the PCB to its upper layer, using a standard PCB process [see Fig. 1(a)]. Next, we complete the antenna structure by wet etching its upper metallization layer. In this second step, the planar sections of the RF MEMS switches (CPW lines) are also formed along with dc bias and dc block circuits [see Fig. 1(b)]. After this structure is obtained, we fab-

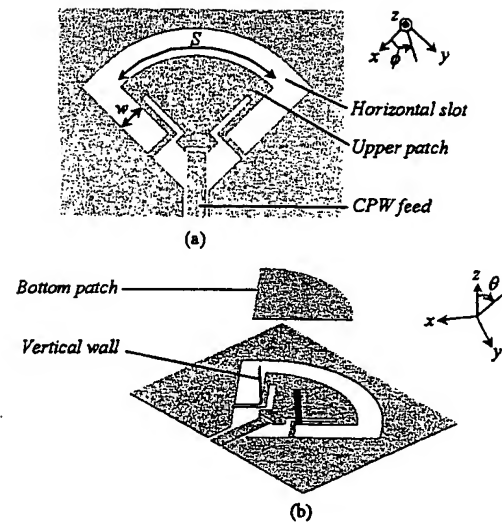


Fig. 2. Schematic of antenna geometry. (a) Top view of the upper layer ($w = 2 \text{ mm}$, $S = 14 \text{ mm}$). (b) 3-D schematic.

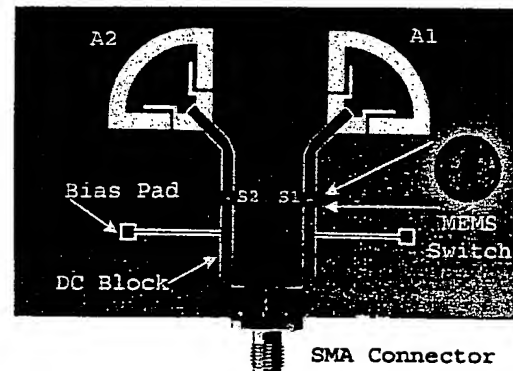


Fig. 3. Photograph of the monolithic RF MEMS switched diversity antenna.

ricate RF MEMS switches following the process flow shown in Fig. 1(c)–(e) without affecting the antenna structure.

Fig. 3 shows the monolithically fabricated RF MEMS-switched diversity antenna. The system consists of two antenna elements and two RF MEMS switches located on CPW feed lines that route the signal to the two antennas. These switches activate either the antenna element for spatial or angular diversity or operate them together to create a superposition radiation pattern for coverage reconfigurability. Antennas are placed at 90° so that, by operating either antenna, orthogonal radiation patterns are obtained. We used high RF impedance quarter-wavelength lines for dc bias to prevent the RF signal from being shorted by the power supply. Similarly, quarter-wavelength dc block circuits isolate the dc bias from the microwave signal (see Fig. 3). These quarter-wavelength dc block circuits run from the RF MEMS switches to the output ports of the tee junction. These lines transform the RF short at the RF MEMS switch locations to an RF open at the output ports of the tee junction. Therefore, when either switch is actuated, the RF signal sees an open at the output port of the tee junction on the actuated side so that it can be directed to either path to sequentially operate the antennas.

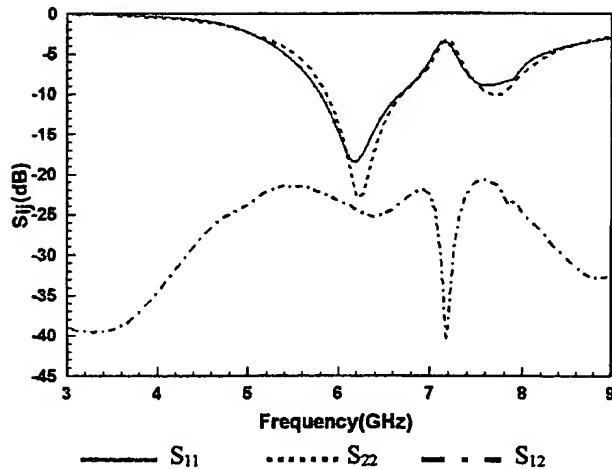


Fig. 4. Measured return loss and mutual coupling for the RF MEMS switched diversity antenna.

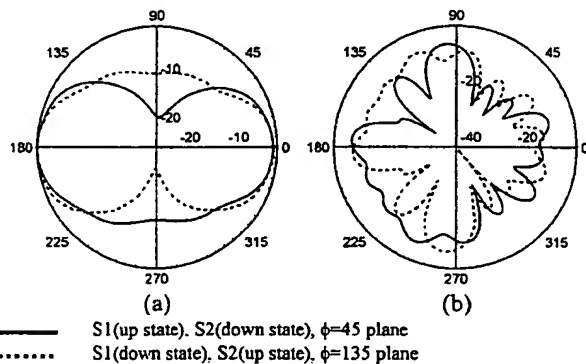


Fig. 5. Measured co-pol. radiation patterns of the RF MEMS switched diversity antenna at 6.15 GHz. (a) In elevation planes: $\phi = 45^\circ$ and $\phi = 135^\circ$ planes. (b) In azimuth plane (x - y -plane).

Fig. 4 shows the measured input impedances of the antenna elements when either switch is actuated, and inter-element coupling corresponding to the simultaneous operation of the antennas (both switches in the up state). The antennas possess 18% bandwidth for a 1:2 voltage standing-wave ratio (VSWR) criteria. For the frequency band of interest, mutual coupling (S_{12}) is below 20 dB, providing low correlation coefficients between radiating elements required for spatial or angular diversity techniques. Fig. 5(a) shows the radiation patterns of each antenna element measured at 6.15 GHz corresponding to the $\phi = 45^\circ$ and $\phi = 135^\circ$ elevation planes. The azimuth patterns of the antennas are given in Fig. 5(b). It is observed that individual operation of antennas (S_1 in the up state, S_2 in the down state, or vice versa) allows covering 180° sectors by switching the beam between antenna elements. These radiation patterns can be employed for spatial or angular diversity techniques to maximize the received signal while minimizing interference.

III. CONCLUSION

RF MEMS technology featuring a novel low-temperature fabrication process has been used to create a monolithically integrated RF MEMS switched antenna system. The system is constructed on an RO4003-FR4 PCB substrate due to its low

cost and widespread use in wireless communication systems. Switching between antenna elements creates different radiation patterns that can, in turn, be employed for different diversity techniques to enhance receiving performance while mitigating multipath effects. Current and future communication systems are likely to benefit from this RF MEMS technology.

ACKNOWLEDGMENT

The authors would like to thank Prof. N. G. Alexopoulos, University of California at Irvine, for helpful discussions and comments on the antenna system.

REFERENCES

- [1] Z. J. Yao, S. Chen, S. Eshelman, D. Denniston, and C. Goldsmith, "Micromachined low-loss microwave switches," *J. Microelectromech. Syst.*, vol. 8, pp. 129–134, June 1999.
- [2] J. B. Muldavin and G. M. Rebeiz, "High-isolation CPW MEMS shunt switches: Modeling and design," *IEEE Trans. Microwave Theory Tech.*, vol. 48, pp. 1045–1056, June 2000.
- [3] N. S. Barker and G. M. Rebeiz, "Distributed MEMS true-time delay phase shifters and wide-band switches," *IEEE Trans. Microwave Theory Tech.*, vol. 46, pp. 1881–1890, Nov. 1998.
- [4] C. L. Goldsmith, A. Malczewski, Z. J. Yao, C. Shea, J. Ehmke, and D. H. Hinzl, "RF MEMS variable capacitors for tunable filters," *Int. J. RF Microwave Computer-Aided Eng.*, vol. 9, no. 4, pp. 362–374, July 1999.
- [5] M. Kim, J. B. Hacker, R. E. Mihailovich, and J. F. DeNatale, "A monolithic MEMS switched dual-path power amplifier," *IEEE Microwave Wireless Comp. Lett.*, vol. 11, pp. 285–286, July 2001.
- [6] A. Singh, D. A. Horsley, M. B. Cohn, A. P. Pisano, and R. T. Howe, "Batch transfer of microstructures using flip-chip solder bonding," *J. Microelectromech. Syst.*, vol. 8, pp. 27–33, Mar. 1999.
- [7] K. F. Harsh, B. Su, W. Zhang, V. B. Bright, and Y. C. Lee, "The realization and design considerations of a flip-chip integrated MEMS tunable capacitor," *Sens. Actuators A, Phys.*, vol. 80, no. 2, pp. 108–118, Mar. 2000.
- [8] B. A. Cetiner, L. Jofre, C. H. Chang, J. Y. Qian, M. Bachman, G. P. Li, and F. De Flaviis, "Integrated MEM antenna system for wireless communications," in *IEEE MTT-S Int. Microwave Symp. Dig.*, 2002, pp. 1333–1337.
- [9] L. Jofre, B. A. Cetiner, and F. De Flaviis, "Miniature multi-element antenna for wireless communications," *IEEE Trans. Antennas Propagat. (Special Issue)*, vol. 50, pp. 658–669, May 2002.
- [10] Rogers Inc., Chandler, AZ, Microwave Products Tech. Information, 2001.
- [11] H. Chang, J. Y. Qian, B. A. Cetiner, F. De Flaviis, M. Bachman, and G. P. Li, "Low cost RF MEMS switches fabricated on microwave laminate PCBs," *IEEE Electron Devices Lett.*, submitted for publication.
- [12] C. H. Chang, J. Y. Qian, B. A. Cetiner, Q. Xu, M. Bachman, F. De Flaviis, and G. P. Li, "RF MEMS capacitive switches fabricated with HDICP CVD SiN_x ," in *IEEE MTT-S Int. Microwave Symp. Dig.*, 2002, pp. 231–234.



B. A. Cetiner (M'00) was born in Famagusta, Cyprus, in 1969. He received the Ph.D. degree in electronic and communication engineering from the Yildiz Technical University, Yildiz, Istanbul, in 1999.

From November 1999 to June 2000, he was a NATO Science Fellow with the University of California at Los Angeles. Since June 2000, he has been with the Electronics and Computer Engineering Department, University of California at Irvine (UCI), where he was a Post-Doctoral Researcher from June 2000 to March 2002. He is currently a Research Specialist with UCI. His current research interest is focused on the analysis and design of microwave circuits, application of MEMS for development of microwave devices, and small size reconfigurable antennas for smart wireless communication systems. He is the inventor of patent-pending printed-circuit-board (PCB) compatible RF MEMS technology.

Dr. Cetiner was the recipient of the 1999 NATO scholarship given by The Scientific and Technical Research Council of Turkey (TUBITAK) for his post-doctoral research.



J. Y. Qian was born in Changsha, China. He received the B.S. degree in opto-electronics and M.S. degree in optics from the University of Science and Technology of China, Hefei, China, in 1994 and 1997, respectively, and is currently working toward the Ph.D. degree in electrical and computer engineering at the University of California at Irvine.

His current research interests include RF MEMS switches and design and analysis of microwave circuits.



G. P. Li developed a silicon silicide molecular beam epitaxy (MBE) system while with the University of California at Los Angeles (UCLA), and then in the area of silicon bipolar very large scale integration (VLSI) technology and process-related device physics while with the IBM T. J. Watson Research Center. During his tenure as a Staff Member and Manager of the Technology Group, IBM, he coordinated and conducted research efforts in technology development of high-performance and scaled-dimension (0.5 and 0.25 μm) bipolar

devices and integrated circuits (ICs), as well as research into optical switches and optoelectronics for ultra-high-speed IC measurements. In 1987, he chaired a committee for defining IBM semiconductor technology for beyond the year 2000. He also led a research/development team in transferring semiconductor chip technology to manufacturing in IBM. In 1988, he joined the University of California at Irvine (UCI), where he is currently a Professor of electrical and computer engineering and Director of the Integrated Nanosystems Research Facility (INRF). He has authored or coauthored over 170 research papers involving semiconductor materials, devices, technologies, polymer-based bio-MEMS systems, RF MEMS, and circuit systems. His current research interests include novel MEMS device design and fabrication for RF wireless communication, biomedical and environmental sensing applications, novel materials and processes for high-speed electronic/opto-electronic device fabrication for network and wireless communication applications, novel electrooptical probing of semiconductor materials, devices, and circuits for *in-situ* wafer quality evaluation and ultra-high-speed chip level testing, and design and fabrication of novel electronic/opto-electronic devices for low-power technology.

Dr. Li was the recipient of a 1987 Outstanding Research Contribution Award presented by IBM and the 1997 and 2001 Outstanding Engineering Professor Award presented by UCI.

H. P. Chang received the B.A. degree in chemical engineering from the National Cheng Kung University, Taiwan, R.O.C., in 1995, the M.S. degree in materials science and engineering from the University of California at Irvine, in 2001, and is currently working toward the Ph.D. degree in materials science and engineering at the University of California at Irvine.

His interests include design, fabrication, and characterization of MEMS systems.



M. Bachman received the Ph.D. degree in experimental physics from the University of Texas at Austin, in 1993.

He is currently an Adjunct Assistant Professor of electrical engineering at the University of California at Irvine (UCI), and Assistant Director of UCI's Integrated Nanosystems Research Facility. He also teaches courses in MEMS and microfabrication at UCI. His research interests address the development of new methods of integrated microsystems engineering for applications beyond microelectronics.

He maintains an active research program in sensors, MEMS, bio-MEMS, and microinstruments for applications in communications and life sciences.



F. De Flaviis received the Ph.D. degree from the University of California at Los Angeles, in 1997.

He became an Assistant Professor with the University of California at Irvine in June 1998. His research has focused on the integration of novel materials and technologies in electromagnetic circuits and antenna systems for the realization of "smart microwave systems." His research is also focused on novel numerical techniques enabling faster codes for the analysis and design of microwave circuits and antennas. His current research is focused on the synthesis of novel

low-loss ferroelectric material operating at microwave frequency, which can be used as phase-shifter design to be employed in scan-beam antennas systems. He is also involved with the modeling MEMS devices to be used as analog tunable capacitors at microwave frequency for the realization of tunable filters, tunable phase shifters, and "smart" matching circuits. Some of his research is also focused on the development of a novel numerical technique in the time domain, which will allow reduction in memory storage and faster computation.